Journal of Structural Geology, Vol. 9, No. 2, pp. 221 to 232, 1987
Printed in Great Britain

0191-8141/87 $03.00 + 0.00

Pressure-solution deformation of the Purgatory Conglomerate, Rhode Island (U.S.A.): quantification of volume change, real strains and sedimentary shape factor

S. MOSHER

Department of Geological Sciences, The University of Texas at Austin, Austin, TX 78712, U.S.A.

(*Received* 18 *April* 1986; *accepted in revised form* 4 *September* 1986)

Abstract—Pressure solution has caused substantial volume redistribution within the Purgatory Conglomerate from Rhode Island. Material has been removed from quartzite cobble surfaces parallel to the fold axes and mostly redeposited as fibrous pressure shadows at the long axis terminations of the cobbles. In the hinges of folds, 23% of the mean cobble volume has been removed, and in highly deformed and overturned fold limbs up to 55% volume reduction has occurred. The initial cobble shape and orientation can be measured at an undeformed locality and the deformation path can be easily deduced; thus these are real cobble volume reductions. Apparent volume losses (initial shapes not removed) range from 70% to 89%. Real strains for cobbles (axial ratios ranging from 1 : 0.65 : 0.38 to 1 : 0.47 : 0.15) have values of e_X, e_Y, e_Z which range from 0%, −20%, −11% to 0%, −37%, −42%, respectively, depending on structural position. The conglomerate itself has been extended parallel to the fold axes (e_x), but the extension is not recorded by the cobble shapes.

INTRODUCTION

THE IMPORTANCE of pressure solution as a deformation mechanism has been debated for over a hundred years (Sorby 1863, Heim 1919, Kuenen 1942, Ramsay 1967, pp. 226–228, Durney 1972, Deelman 1975, McClay 1977, De Boer 1975, 1977). Although pressure-solution deformation is now widely recognized in carbonates (Nickelsen 1972, Geiser 1974, Alvarez *et al.* 1978), quartzites (Elliott 1973, Mitra 1977), conglomerates (Mosher 1976, 1978, 1980, 1981, McEwan 1978), slates (Von Plessmann 1964, Wood 1974, Geiser 1979, Wright & Platt 1982) and crenulated schists (Gray 1978, Gray & Durney 1979), the volume of material which can be redistributed by this mechanism is still unknown, primarily because of the lack of natural strain indicators with known original volumes. Fossils can be used (e.g. Nickelsen 1966, Engelder & Engelder 1977, Geiser 1979). However, their usual scarcity allows only local estimates which do not necessarily reflect the bulk volumetric strain. One study using abundant graptolites in slates yields estimates of bulk volume losses (50%) during cleavage formation (Wright & Platt 1982); however, the amount of volume reduction due to pressure solution cannot be separated from that caused by post-lithification, tectonically-induced dewatering of the clay minerals or other volume-changing processes affecting shales discussed by Ramsay & Wood (1973, p. 271).

Use of other natural strain indicators such as reduction spots (Ramsay & Wood 1973, Wood 1974) and conglomerate clasts (Mosher & Wood 1976, 1978, Mosher 1977, 1978) for calculation of volume change involves assumption of initial sphericity and/or plane strain. In both cases such assumptions lead to unreasonably high estimates of volume change or redistribution (Ramsay & Wood 1973, Mosher & Wood 1976). Recently, discrete zones of deformation within rocks (e.g. shear zones, limbs of crenulation cleavages, deformed matrix around rigid objects) have been used to calculate apparent volume change. These estimates rely on models for ideal band development (see Schwerdtner 1982) or on determination of the amount of insoluble material concentrated within these zones (e.g. Gratier 1983). Application of the former has generally led to geologically unrealistic values for volume change (Grunsky *et al.* 1980, Schwerdtner 1982, Mawer 1983), and the many problems inherent in the latter method (Mosher 1978, 1981) suggest such results should only be used for qualitative comparisons.

The effects of ductile deformation can be quantified by calculating the magnitude of finite strain from the shapes of natural strain indicators, originally semi-spheroidal objects such as ooliths, spherulites, vesicles, amygdales, reduction spots, accretionary lapilli and conglomerate clasts (e.g. Sorby 1853, Cloos 1947, Flinn 1956, 1962, Ramsay 1967, Gay 1968, Hossack 1968, Helm & Siddans 1971, Wood 1973, Milton & Chapman 1979, Ribeiro *et al.* 1983, Siddans 1983). The use of natural strain indicators requires comparison of the measured deformation ellipsoid axes with some original shape parameter. One approach assumes that one axis of the ellipsoid remains constant (Cloos 1947, Mosher & Wood 1976); another assumes the diameter of an equal volume sphere is equivalent to the original diameter (Flinn 1956, Hsu 1966, Ramsay 1967, pp. 136–137, Wood 1973, 1974). Both approaches rely on either assumption or determination of original sphericity (Wood 1974, Wood & Oertel 1980). The latter also requires no volume change during deformation. In most cases both assumptions are invalid (Wood 1974), and methods have been postulated for determining either the original shapes (Ramsay 1967, Dunnet 1969, Elliott

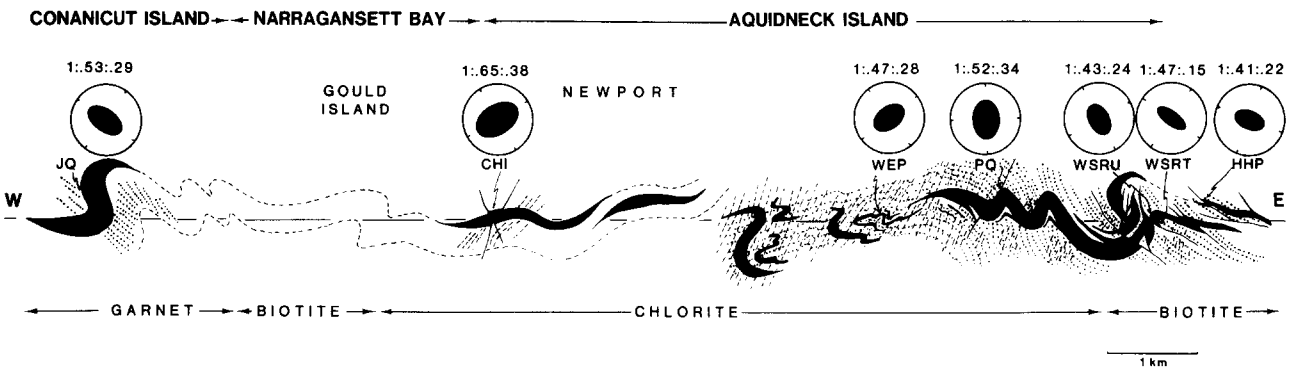

Fig. 1. Profile across southeastern Narragansett Basin through the Purgatory Conglomerate outcrops (solid black). [First cleavage dotted (shallow), second dashed (steep).] The ellipses show lengths [relative to a constant long (X) axis dimension] and orientations of intermediate (Y) and short (Z) axes of the cobbles which are found in the plane of the profile. The circles represent the dimension of the long axis relative to the other two axes; long axes are oriented perpendicular to the plane of the profile. Structure in the fine-grained rocks (dashed layers) exposed from Gould Island to the western edge of profile has been greatly simplified, and the profile only shows the structural position of the JQ locality relative to other localities.

1970, Dunnet & Siddans 1971, and others) or the amount of volume reduction (Ramsay & Wood 1973, Mosher & Wood 1976). Corrections for original shape factor, however, assume a constant volume for the strain marker, and methods correcting for strain determinations involving volume loss assume initial sphericity so that for the general case of strained, non-spherical objects with volume loss, neither method can be strictly applied. The actual effects of either or both assumptions on strain calculations using natural strain indicators have not been documented, because real strain can rarely be determined. To calculate real strain from natural indicators, the deformation mechanism, the initial clast shape and axial orientation, and the deformation path must be known.

This paper presents the results from a study of the Purgatory Conglomerate from the Narragansett Basin of Rhode Island, U.S.A. The conglomerate provides an unusual opportunity to measure volumetric strain. The only deformation mechanism that affected cobble shapes is pressure solution (Mosher 1976, 1978, 1981), and original cobble shapes and axial orientations are known. In addition, the deformation path can be easily deduced because of the presence of an undeformed locality. Thus, the amount of volume redistribution and real finite strain can be determined.

Conglomerate composition, structural setting and deformation mechanism

The Purgatory Conglomerate is part of a large alluvial fan complex which formed off the eastern margin of the Pennsylvanian-age Narragansett Basin of Rhode Island (Mosher 1978, 1983). The main conglomerate unit is approximately 135 m thick, and lenses of the conglomerate extend across two-thirds of the basin. The unit is a massive, poorly-sorted conglomerate composed predominantly of quartzite clasts. Little matrix is present, and the conglomerate is entirely clast-supported. Clasts are approximately triaxial ellipsoids with arithmetic mean axial ratios ranging from 6.7:3.1:1 to 2.6:1.7:1. Clast size varies greatly with lengths ranging from 1 cm to 1.8 m; average clast length is approximately 30 cm. Most clasts fall in the cobble size range, so will hereafter be referred to as cobbles. Conglomerates deposited in alluvial fan environments usually have a sedimentary fabric. The long/intermediate axis planes lie subparallel to bedding and the long axes are oriented transverse to flow (Rust 1972, Walker 1975). For the Purgatory Conglomerate, flow was westward off N-trending basin margins, hence long clast axes should trend northward if the conglomerate is undeformed.

The main conglomerate unit occurs in N-trending overturned W-vergent folds with wavelengths of 0.7 km (Mosher 1978, 1981) (Fig. 1). Associated W-directed thrusts deform the conglomerates near the eastern basin margin (Mosher 1978, 1980). The thrusts and the axial surfaces of the folds are broadly warped by a later coaxial folding which deformed the thin distal ends of the conglomerate and the finer-grained basin sediments into tight, E-vergent folds (Farrens 1982) (Fig. 1). Normal and strike–slip faulting and boudinage followed folding (Mosher 1983).

The conglomerate was deformed by pressure solution and inter-cobble rotation during the first two folding events (Mosher 1976, 1981). Intracrystalline plastic deformation did not affect the cobbles (Mosher 1976, 1981). Long cobble axes are aligned parallel to the fold axes, and fibrous quartz pressure shadows are present at the long axis terminations (Fig. 2), indicating bulk extension parallel to fold axes. Original cobble margins may still be distinguished. All other cobble surfaces are indented (Fig. 3), indicating removal of material. Hence, cobble axes perpendicular to fold axes have been shortened, and the original cobble axes parallel to fold axes have remained unchanged. Planes containing the long and intermediate cobble axes define a rough axial planar foliation. It should be noted that the fold axes are parallel to the N-trending basin margins, hence the long cobble axes are parallel to the original long axis orientation predicted from the depositional setting.

Cobble deformation associated with thrusting was

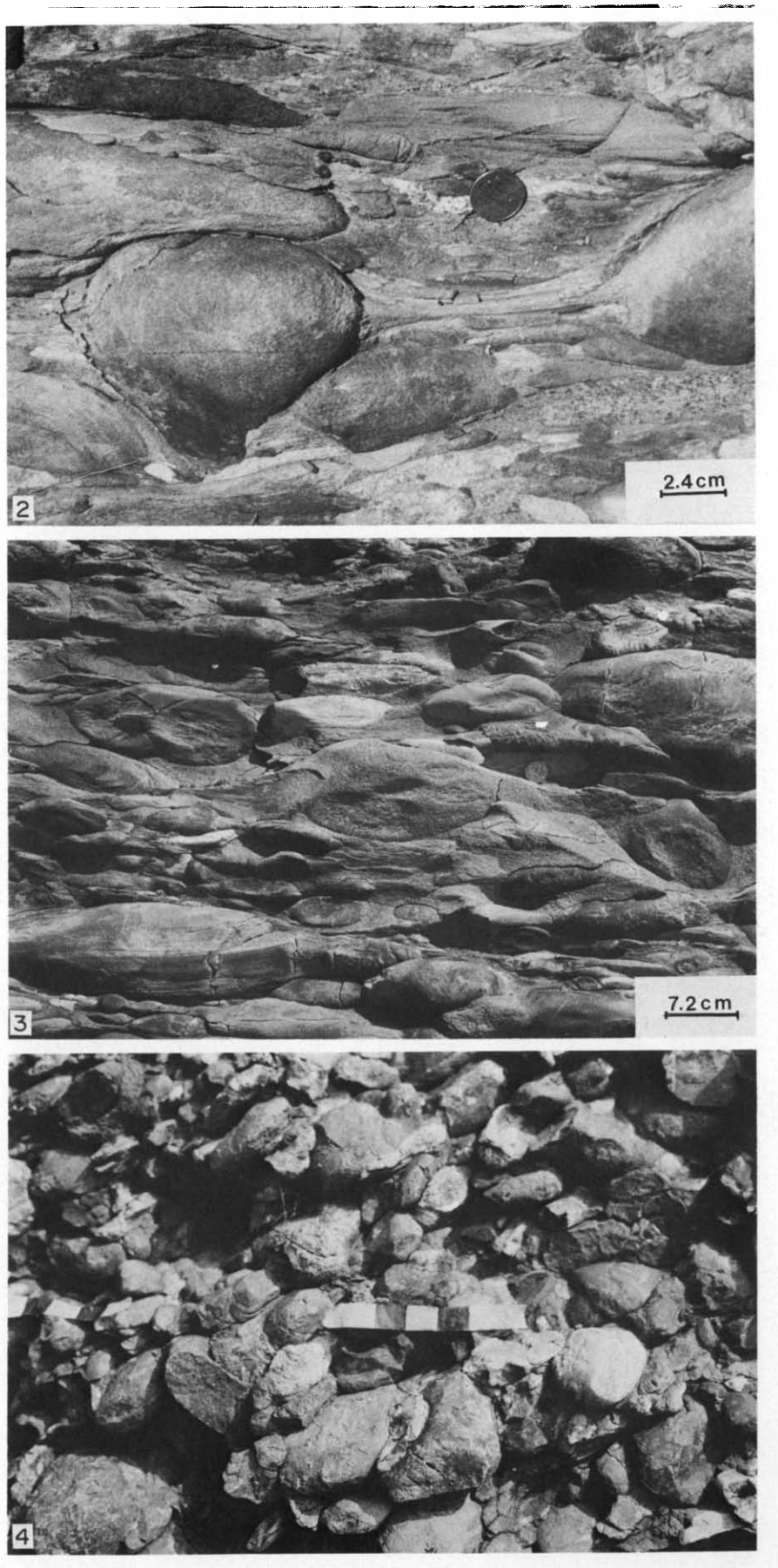

Fig. 2. Long fibrous quartz pressure shadows are found connecting long (X) axis terminations of adjacent cobbles.

Fig. 3. Many indentations cover cobble surfaces that are subparallel to the fold axes. Cobble long axes show a strong preferred orientation.

Fig. 4. Undeformed conglomerate at CHI; note irregular shapes and lack of cobble axis alignment. Bars are 2.5 cm in length.

also by pressure solution, although cobbles in one intensely deformed shear zone have also been affected by extensional fracturing and possible intracrystalline plastic deformation (Mosher 1980). Late-stage normal and strike–slip faulting and boudinage produced only local brittle deformation of the conglomerate and had no effect on the cobble shapes or orientations.

Most of the conglomerate, which is located in the SE portion of the basin, was metamorphosed to lower greenschist facies after the pressure-solution deformation (Mosher 1978, 1981). The conglomerate located in the SW portion of the basin was affected by upper amphibolite facies metamorphism which culminated earlier, apparently allowing less time for pressure-solution deformation.

Location of strain analyses

Eight localities, in different structural situations and metamorphic grades, were selected for strain analyses (see Table 1 and Fig. 1). At each locality over 100 adjacent cobbles were individually removed, and lengths and orientations of cobble axes were measured. Cobbles of uniform long axis lengths were selected for all localities except WEPL where all clasts fall in the pebble size range. The arithmetic mean axial ratios (indicative of final cobble shapes) of each locality are given in Table 1 and are represented on the profile in Fig. 1. Throughout this paper, the convention $X \geq Y \geq Z$ will be used for cobble axes.

Undeformed locality

The locality, CHI, is comprised of gently tilted beds capping the top of a rigid basement horst. Virtually no evidence of cobble deformation, including pressure solution, is observed (Fig. 4). Long and intermediate cobble axes lie subparallel to bedding, and the majority of long cobble axes are oriented within 30° of the N-trending basin margins (Fig. 5). Nevertheless, this alignment of long cobble axes, relative to one another and to the N-trending fold axes, is poor, when compared to those at the deformed localities. The orientations of CHI cobble axes are, however, consistent with the expected original sedimentary fabric for this conglomerate which suggests that in addition to being undeformed, conglomerate clasts have not been appreciably reoriented by the later deformation. Comparison of CHI with an undeformed

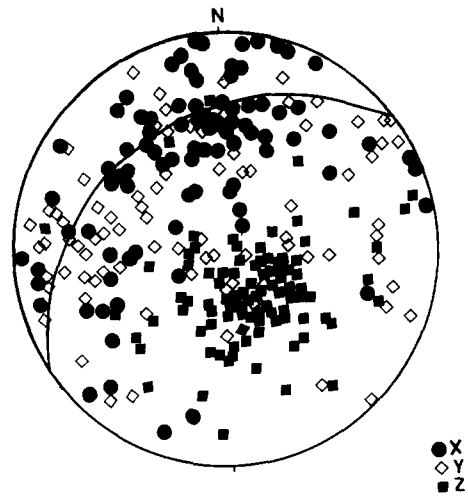

Fig. 5. Stereonet showing orientation of cobble axes at CHI. Bedding (indicated by solid line) has a dip of 22°NW. Most long and intermediate axes lie in the plane of the bedding. Long (X) axes are concentrated in the north.

Table 1. Real strains and volume changes for cobbles

Locality (from east to west)	JQ	CHI	WEP	WEPL	PQ	WSRU	WSRT	HHP
Structural situation	Overturned limb, first fold	Gently tilted beds	Upright limb, second fold	Same location as WEP, matrix supported pebble conglomerate	Hinge, upright first fold	Overturned limb, first fold, within 25 m wide shear (thrust) zone	Core of 2 m wide thrust zone, overturned limb*	1 m wide thrust zone, right side up limb of overturned first fold
Metamorphic grade	Garnet	Chlorite	Chlorite	Chlorite	Biotite	Biotite	Biotite	Biotite
Mean axial ratios								
Arithmetic	1/.53/.29	1/.65/.38	1/.47/.28	1/.43/.25	1/.52/.34	1/.43/.24	1/.47/.15	1/.41/.22
Tectonic strain ratios (shape factor removed)	1/.81/.74	1/1/1	1/.72/.74†	1/.66/.66	1/.8/.89†	1/.66/.63	1/.72/.39	1/.63/.58
Real strain (shape factor removed) (% elongation)	X Y Z 0 −19 −26	X Y Z 0 0 0	X Y Z 0 −28 −26	X Y Z 0 −34 −34	X Y Z 0 −20 −11	X Y Z 0 −34 −37	X Y Z 0 −28 −61*	X Y Z 0 −37 −42
Volume change (%)								
Real (shape factor removed)	−35	0	−41	−45	−23	−48	−65*	−55
Apparent (spherical)	−80	−70	−82	−83	−77	−84	−89	−86

* WSRT is 1 m from WSRU; some non-pressure-solution deformation has occurred; see text and Mosher (1980).
† Ratios given in final axis order $X_F/Y_F/Z_F$. Note here tectonic order is $X_T/Z_T/Y_T$ as Z_T paralleled Y_F and Y_T paralleled Z_F.

conglomerate in New Mexico, which was also deposited in an alluvial fan complex, further supports the conclusion that CHI is relatively undeformed (Houle 1980). The two conglomerates have similar sedimentary fabrics and an identical mean cobble shape (Houle 1980). The cobble shapes at CHI are therefore considered to be in an original, undeformed state. The clasts at this undeformed and the deformed localities are the same composition, have the same source, and were deposited in an alluvial fan complex by the same processes. Thus, the original range of shapes, the shape distribution, and the sedimentary fabrics should be equivalent, and the CHI locality may be considered the original undeformed state of the deformed conglomerate. Any difference in size distribution is unimportant because axial ratios or normalized data are used throughout.

STRAIN

Removal of initial shapes

Tectonic strain can be determined by removing the effects of the initial shapes from the final shapes. However, both original cobble shapes and axial orientations must be known. The importance of the relationship between final and original axial orientations is illustrated in Fig. 6. In case A, the Y_O axis should be removed from the X_F axis, and the X_O from the Y_F. If X_O is assumed parallel to X_F and Y_O to Y_F, an incorrect strain is determined. In case B, the assumption of parallelism is valid, and a correct strain is determined. The relationship between original and final axial orientations can be found by comparing the present relationships between undeformed and deformed cobble axial orientations and

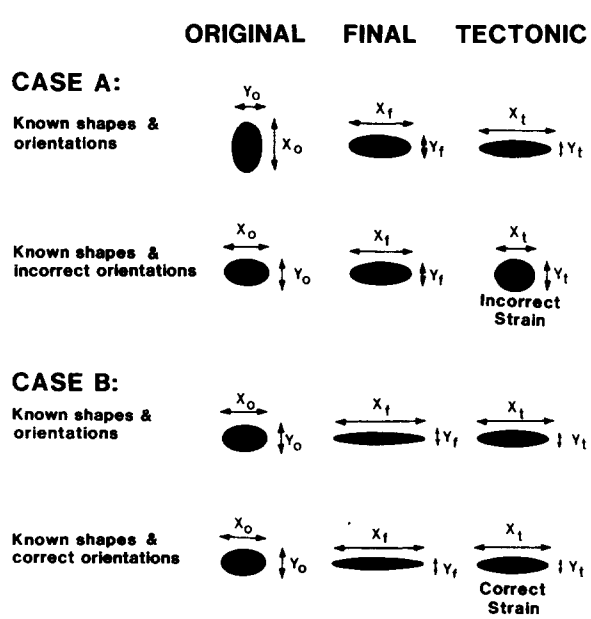

Fig. 6. Importance of relationship between original and final axial orientations; comparison of correct (real) strains and those calculated assuming X_O parallels X_F, Y_O parallels Y_F. Case A, parallelism assumption invalid; case B, parallelism assumption valid.

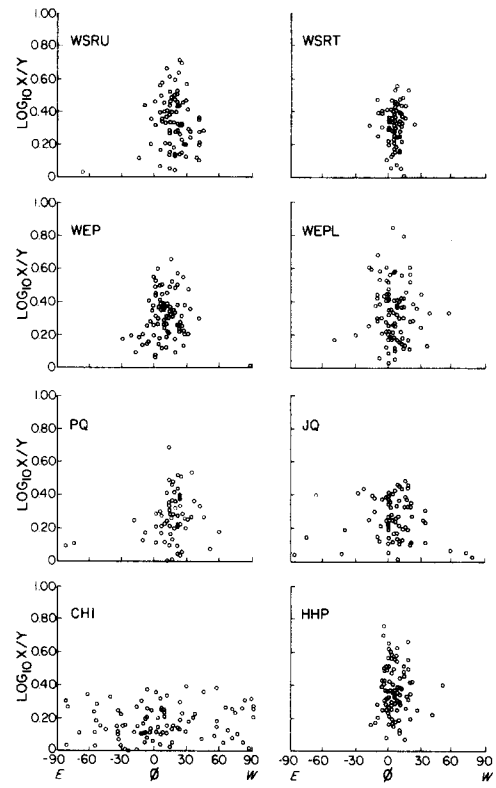

Fig. 7. R_f/ϕ plots for the XY cobble plane; fold axes trend 008–014°N. The fluctuation of the X axes from each other and from the fold axes is minor for all deformed localities. CHI (undeformed locality) shows a large fluctuation but the majority of the long axes are in the same orientation as those in the other localities.

by considering the deformation path to ascertain whether the cobbles axes have changed orientation during deformation, and if so, in what manner. In this section axial orientations of cobbles from the undeformed locality are compared with final orientations of cobbles from the deformed localities. The original and final cobble shapes and deformation mechanisms are then discussed to determine the deformation path and hence the relationship between original and final axes. Finally, original shapes are removed from the final shapes at deformed localities to produce tectonic strain ratios.

Axial orientations at deformed localities are best compared with those at the undeformed locality CHI using R_f/ϕ plots (Ramsay 1967, pp. 209–221) (Figs. 7 and 8). All deformed localities show good alignment of X cobble axes with fold axes in the XY plane; a similar plot for locality CHI shows poor alignment (Fig. 7). Statistical comparisons of original X axis orientations (CHI) with final orientations (deformed localities) show 76% of original X axes are aligned within 30° of final X axes orientations (see also Fig. 5). R_f/ϕ plots in the YZ plane (Fig. 8) show poor alignment of Y axes with bedding at the deformed localities and relatively good alignment at CHI. Although not shown by the R_f/ϕ plots, the XY plane of the cobbles forms an axial planar cleavage in the field at deformed localities. (Note that methods using R_f/ϕ plots to remove sedimentary fabric are not applicable in this case because the strain markers change volume during deformation.)

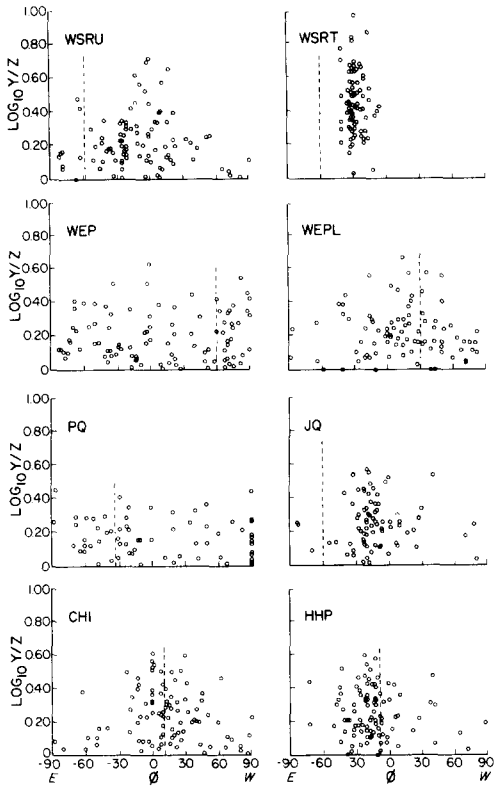

Fig. 8. R_f/ϕ plots for the YZ cobble plane. The trace of bedding is a dashed line. For CHI most Y axes parallel bedding; for overturned localities (WSRU, WSRT, JQ) Y axes are shallower than bedding and form tight clusters; at right-way-up localities (HHP, WEP, PQ) most Y axes are steeper than bedding.

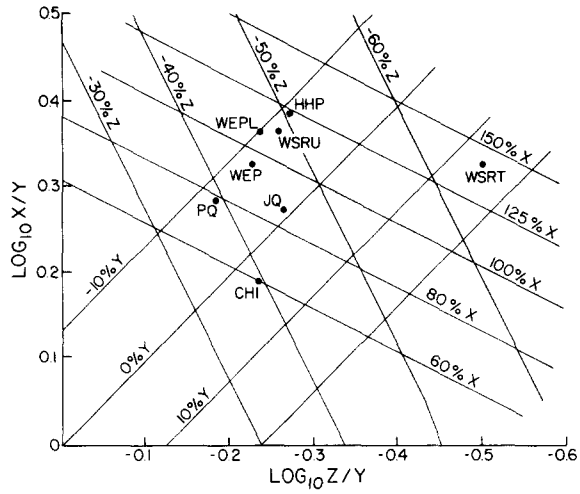

Fig. 9. Summary deformation plot of arithmetic mean cobble shape for each locality. Axial shortenings are indicated using the plot of Wood (1974) and are given relative to diameter of initial sphere.

Differences between original and final shapes are best shown on a Flinn (1956) plot (Fig. 9). The majority of cobble shapes and the mean cobble shape are oblate for CHI and are prolate for six deformed localities. In addition, cobbles become more prolate as volume loss increases (CHI to PQ to JQ to WEP to WEPL to WSRU to HHP as shown in Table 1; see next section for calculation of volume change). Hence, folding deformation was constrictional, substantially shortening one axis of oblate cobbles. (Note that although the cobble long axes do not change in length, extension of the conglomerate as a whole does occur parallel to fold axes as shown by the fibrous pressure shadows. Thus, cobbles underwent plane strain, whereas the bulk conglomerate strain is truly constrictional.) The pronounced oblate shape of cobbles at WSRT reflects superimposed fracturing (and possible intracrystalline plastic) deformation which occurred at that locality during thrusting (Mosher 1980). Only this intense shearing (WSRT) caused sufficient flattening to overprint the constrictional strain.

The deformation mechanisms during folding were pressure solution, which changed the cobble shapes, and inter-cobble rotation which reoriented the cobble axes. Field and petrographic relationships (Mosher 1976, 1981) support continuous removal of material by pressure solution throughout folding.

The deformation path can be deduced by considering the present relationships between deformed and undeformed cobble axial orientations, the differences between undeformed (original) and deformed (final) cobble shapes, and the deformation mechanisms. During folding, inter-cobble rotation (rigid body rotation) caused the plane containing the X and Y cobble axes to rotate toward parallelism with fold axial surfaces. This plane also rotated with bedding during folding because it was originally subparallel to bedding. The effects of both rotations on cobble orientations within the YZ plane during folding are shown in Fig. 10 for five representative cobbles. One result is that on right-way-up fold limbs, the cobble XY plane dips in the same direction as the beds but steeper, and on the overturned limbs, is shallower. This relationship exists for all of the seven deformed localities (Fig. 8). Additionally, inter-cobble rotation caused original X axes which were oriented within 30° of the fold axes to rotate toward parallelism with the fold axes (Fig. 11). Seventy-six per cent of the original X axes fall in this category and are now parallel to the final X axes.

As fold limbs and cobbles rotated with respect to the stresses during folding, material was removed from surfaces parallel to the fold axial surfaces (Fig. 10). No indentations are found on surfaces perpendicular to the final long axes, so no shortening occurred in this direction (Fig. 11). The continuous shortening of cobble dimensions perpendicular to the fold axes caused the final prolate cobble shapes. Three categories of cobbles were affected as follows: (1) spheroidal cobbles became ellipsoidal with long axes parallel to the fold axes; (2) ellipsoidal cobbles with long axes that had rotated into parallelism with, or that were already aligned parallel to, the fold axes (~76%) became more ellipsoidal, and (3) ellipsoidal cobbles with original long axes oriented at angles greater than 30° to the fold axes (<24%) had the original X axes shortened. For these few cobbles, the shortened original X axes may be the final Y axes or may have rotated toward the fold axes to become final X axes. The difference between the lengths of these few original and final X axes is slight and can be ignored if the arithmetic mean axial ratio for all CHI cobbles is used

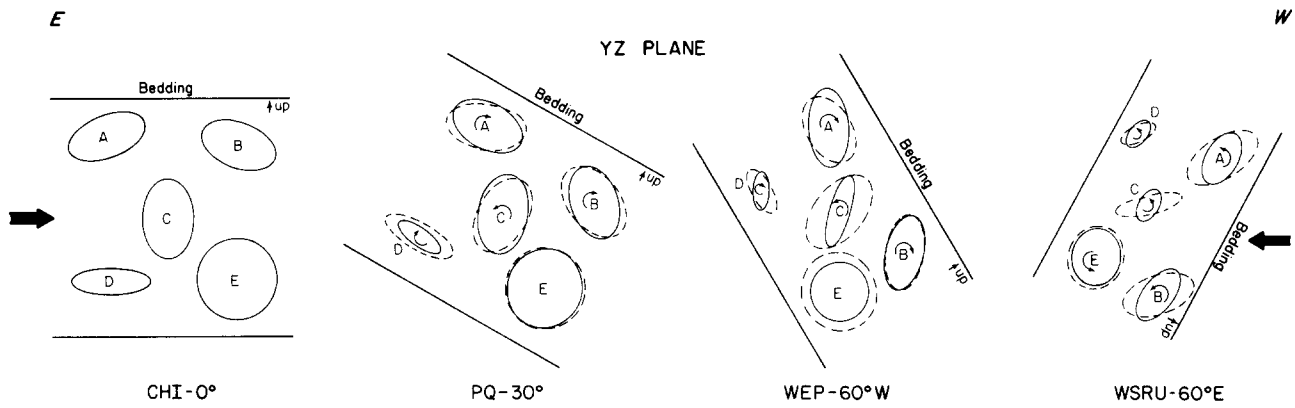

Fig. 10. Progressive changes in cobble shapes and orientation within the YZ plane during folding. Bedding changes in dip from 0° to 30° to 60° to overturned 60°. The shapes and orientations of cobbles A–E were derived from data for localities with the same dips (Fig. 8). (Note dip direction for PQ was changed.) Cobbles A and B represent the mean cobble shape and average fluctuation of Y axes from bedding at each location; cobble C, the most elliptical shape with a Y axis perpendicular (CHI) or at a high angle (deformed localities) to bedding; cobble D, the most elliptical shape with a Y axis parallel (CHI) or nearly parallel (deformed localities) to bedding; cobble E represents the tectonic strain ratio. Dashed ellipses show shape and orientation of cobbles if *only* rotation with bedding, solid ellipses show shape and orientation if pressure solution affects surfaces perpendicular to maximum compressive stress (large solid arrows) and if the XY plane of cobbles rotates toward the fold axial surfaces (curved arrows show direction of rotation). Trace of axial surface for right-way-up beds is steeper than bedding, for overturned, shallower. When beds overturn, cobbles A, B and D change direction of rotation. The change in spacing between bedding planes is proportional to the mean shortening measured in the Z direction. Note the constrictional nature of the deformation (cobble E).

for comparison with the deformed localities because (1) the original X/Y axial ratios never exceed 2.5 : 1 and (2) the most ellipsoidal cobbles should show the best sedimentary alignment (i.e. N-trending, which also parallels the fold axes).

For this conglomerate, therefore, the original axes are, for the most part, parallel to the same axes in the final state ($X_O \parallel X_F$, $Y_O \parallel Y_F$, $Z_O \parallel Z_F$; Fig. 6, case B). The Y and Z axes were reoriented and shortened, and the X somewhat reoriented. The parallelism of the same final and original axes is consistent with the sedimentary environment and fold axis orientation. (Note that the method used above of determining the relationship between the original and final axes is valid regardless of which original and final axes are parallel.)

The original shape factor can now be correctly removed from the final shapes by dividing the final (measured) axial ratios by the originals (Ramsay 1967, pp. 209–211). Mean axial ratios are used because large numbers of strain markers were analysed at each locality. The arithmetic mean of the measured original and final axial ratios gives a true measure of the original and final shapes, whereas harmonic means of the axial ratios more closely approximate the tectonic strains (Lisle 1977, Ramsay & Huber 1983, p. 80). Hence, the arithmetic mean axial ratios are used in removing the original shape factor. Resulting tectonic strain ratios are given in Table 1. These ratios show the constrictional nature of the deformation and suggest that much pressure solution occurred early in the deformation. The three localities

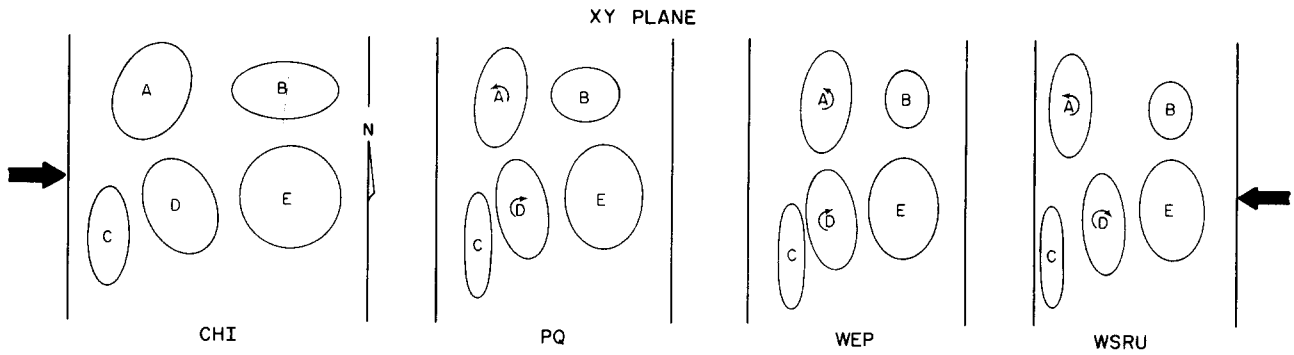

Fig. 11. Progressive changes in cobble shapes and orientations within the XY plane during folding. Bedding changes in dip as shown in Fig. 10; note the XY plane is also rotating in space (not shown). The shapes and orientations of cobbles A–E were derived from data for localities with the same dips (Fig. 7). Cobbles A and D represent the mean cobble shape and average fluctuation of X axes from the fold axes (here shown as N-trending) at each location; cobble C, the most elliptical shape with its X axis parallel to the fold axis; cobble B, the most elliptical shape with its X axis perpendicular to the fold axis (CHI, PQ) and the least elliptical shape with X parallel to the fold axes (WEP, WSRU; at these localities, no cobbles have X perpendicular to the fold axes; see Fig. 7); cobble E shows the change in shape from a circle. Note the dimension parallel to the fold axes (X direction except for cobble B) is unchanged in *all* cobbles. Pressure solution affects surfaces perpendicular to maximum compressive stress (large solid arrows); X axes rotate toward the fold axes (curved arrows show direction of rotation). The change in spacing between N-trending lines is proportional to the mean shortening measured in the Y direction. Note the pronounced decrease in shortening in the Y direction as folding progresses and the XY plane rotates toward parallelism with the fold axial surfaces (Fig. 10).

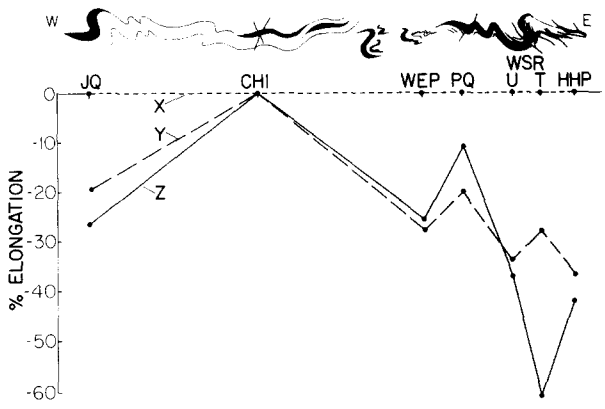

Fig. 12. Real strains (shape factor removed) for seven localities plotted against the distance between localities as shown on the profile (also see Fig. 1). Note in the least deformed areas (PQ and WEP) shortening of Y is greater than of Z, whereas in the most deformed areas (JQ, WSRU, HHP, WSRT) shortening of Z is greater than of Y.

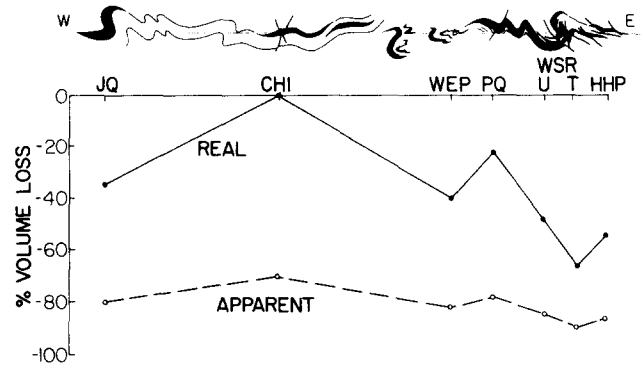

Fig. 13. Real and apparent (shape factor not removed) volume change for seven localities. Volume changes are plotted against the distance between localities as shown on the profile (also see Fig. 1).

from an upright fold show $Z_{TECTONIC}$ is parallel to Y_{FINAL} and therefore to $Y_{ORIGINAL}$ (WEP, limb; PQ, hinge), or $Y_{TECTONIC}$ is equal to $Z_{TECTONIC}$ (WEPL, limb). Thus the axis originally within bedding ($Y_{ORIGINAL}$) has been shortened the most.

Real strain

Real strains are calculated for each locality using the *tectonic* strain ratios calculated above. For this conglomerate, the X axis of the ellipsoids remained constant during deformation. After removal of the original shape factor, the resulting dimension in this axial direction is equivalent to the original spherical diameter of the strain ellipsoid. Thus, the percentage shortening of each axis can be calculated directly from the tectonic (original shape factor removed) strain ratios of Y/X and Z/X (Mosher & Wood 1976). Real strains vary from $e_X = 0$, $e_Y = -0.20$, $e_Z = -0.11$ to $e_X = 0$, $e_Y = -0.37$ $e_Z = -0.42$. Values for each locality are given in Table 1 and are plotted versus structural position in Fig. 12.

The original Purgatory Conglomerate clasts were sufficiently ellipsoidal that the large strains observable in the field are for the most part, apparent strains. Real strains are moderate as might be expected by a pressure-solution deformation mechanism. Small axial strains, however, can produce significant volume changes as is shown below. Again it must be noted that these strains are for the cobbles themselves and that the conglomerate as a whole underwent extension parallel to the fold axes. Thus the real strain of $e_X = 0$ for the cobbles does not represent the bulk strain (e_X) for the conglomerate.

VOLUME CHANGE

Volume changes can be determined for the Purgatory Conglomerate because no material has been removed from the long (X) axis and any addition of material (i.e. pressure shadows) is detectable and removable. Volume change $[(V_F - Vo)/Vo]$ is determined by comparing final and original ellipsoidal volumes. The mean cobble volume of a large number of cobbles is used for each locality. Mean cobble volumes are calculated using normalized values of the cobble dimensions to allow comparison with the volume of an original ellipsoidal mean cobble volume. At each locality, dimensions of individual cobbles are normalized to the unchanged axis (i.e. $X = 1$), and the volume of each cobble is calculated from the normalized dimensions. The arithmetic mean of these normalized volumes is the mean cobble volume for each locality.

In this paper, the mean cobble volume at CHI is used as the original ellipsoidal volume. Three assumptions are made when using CHI. (1) During deformation the X axis remains constant. (2) The original and final X axes remain parallel. This assumption is required because the deformed and undeformed X axes are equated when calculating the volumes from the axial ratios. (3) The range of shapes and the shape distribution were the same at all localities prior to deformation. Any difference in size distribution is accounted for by the normalization process.

Real cobble volume losses, calculated by comparing the mean volume of CHI cobbles with the mean cobble volumes for the seven deformed localities, vary from 23% to 55% (Table 1). Real changes in mean cobble volume are plotted against structural situation in Fig. 13. The amount of cobble volume removed reflects differences in structural situation. The fold hinge locality (PQ) shows the least volume loss, whereas fold limb localities (JQ, WEP, WEPL) show nearly twice as much cobble reduction. More volume loss occurs in thrust-related shear zones (WSRU, HHP, WSRT); the intensity of shearing is reflected by the amount of volume loss (Mosher 1980). [Note that the 65% reduction calculated for WSRT is not a real volume change because other deformation mechanisms affected the cobbles; see Mosher (1980).] Also shown in Fig. 13 for comparison are apparent cobble volume reductions (70–89%, Table 1) calculated using an initial spherical volume. Clearly initial shape factor has a significant effect on volume change calculations.

In the above analyses, means of normalized cobble volumes (i.e. volumes calculated from normalized

dimensions) are used. If all localities had the same number of X axes of a given length as the undeformed locality CHI, then direct comparisons of the *absolute* cobble volumes at CHI and each deformed locality would be possible. Such a situation is unlikely and, because normalized axial lengths are used, the results given in Table 1 depend only on CHI having the same shape distribution as the original conglomerate had at each deformed locality. Three localities, however, have distributions of X-axis-length frequencies that are similar to CHI. Thus a comparison of absolute cobble volumes at these three localities with those at CHI provide a test of the above analyses. Volume losses using normalized and absolute volumes, respectively, are: WEP, 41.2% and 40.7%; JQ, 35% and 38%; WSRU, 48% and 46%, strongly supporting the validity of the normalization process and assumptions used to calculate volume changes.

Real cobble volume losses calculated for the Purgatory Conglomerate demonstrate the importance of the pressure-solution deformation mechanism; large volumes (23–55%) of material can be redistributed in response to nonhydrostatic stresses. Rough mass-balance estimates at WEP show at least 83% of the removed cobble material was locally redeposited as a quartz-rich matrix or fibrous pressure shadows at the long (X) axis terminations of the cobbles. Much of the remaining material can be found in fibrous quartz veins which are ubiquitous throughout the basin sediments and adjacent basement rocks. Because much of the material is redeposited, the bulk strain for the conglomerate will differ from that measured using the cobbles. Cobble strain of $e_X = 0$ measured parallel to the fold axes (X direction of cobbles) will represent a minimum value for the conglomerate. Bulk strain for the conglomerate has a component of extension parallel to the fold axes as indicated by the pressure shadows.

QUALITATIVE STRAIN PATH

Some indication of the successive incremental strains or the strain path is given by the finite strains measured for different structural situations. If the conglomerate in one structural position progressed through other structural positions to reach its present state, then the strains measured for the conglomerate in these other positions may roughly correspond to earlier strain increments in a progressive deformation. For example, overturned fold limbs (WSRU) were once upright (WEP) and some time prior to that were nearly horizontal but compressed, similar to conglomerate layers in present fold hinges (PQ) (Figs. 10 and 11). Thus a possible strain path for the Purgatory Conglomerate can be drawn by connecting the strains measured at these localities going from the undeformed locality, CHI, through PQ, WEP, and finally WSRU (Fig. 14). Of course this path is not quantitative (or strictly correct) because deformation of clasts in hinges and upright limbs continued while limbs were overturning. Hinge regions, however, generally

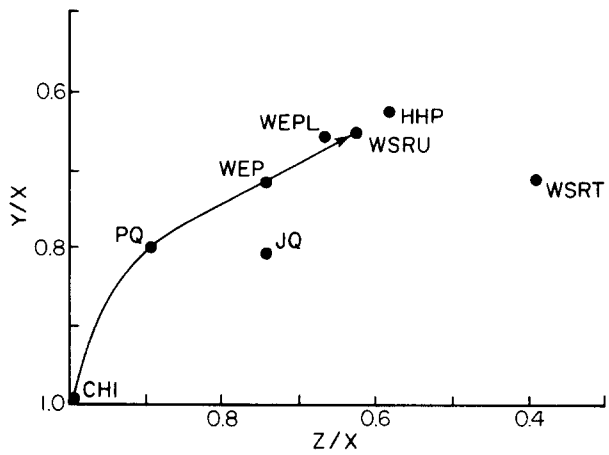

Fig. 14. Possible strain path plotted on summary deformation plot of Mosher & Wood (1976). Points represent the tectonic strain ellipsoids for each locality. The amount of shortening is calculated by subtracting the values from 1.0 because the X dimension is unchanged.

show less strain than limbs, and the overall path gives at least an approximation of the incremental strain path.

The general deformation path discussed previously showed that most cobbles were originally oblate and became prolate during folding as material was removed from all sides of the cobbles except those perpendicular to the fold axes. If a strain path is drawn connecting the mean values for real strains on Fig. 14, the path suggests that at first the Y axes underwent more shortening than the Z axes. As folding progressed, both the Y and Z axes were shortened, but Z more than Y. This strain path is reasonable because: (1) Y axes originally were parallel to bedding and would be affected by layer-parallel compressive stress first; (2) cobbles rotated with bedding during folding causing removal of material off all surfaces except those perpendicular to X; and (3) the XY plane of the cobbles rotated rigidly into axial surfaces of the folds causing more shortening of the Z axes during late stages of folding. The strain path also suggests that most of the pressure solution occurred prior to and during the beginning stages of folding. This conclusion is supported by the parallelism of Z_{TECTONIC} and Y_{FINAL} for upright fold localities, as previously mentioned, and by petrographic evidence that suggests some pressure solution occurred prior to folding (Mosher 1976).

Three localities do not fall on the strain path discussed above. The locality (HHP), on the upright limb of an overturned fold, has undergone slightly more strain than its overturned counterpart (WRSU). This difference reflects the nearly horizontal attitude of the beds (e_Y larger) and an increase in intensity of shearing (e_Z larger). The intense thrust zone locality (WSRT) was affected by other deformation mechanisms (Mosher 1980), and thus should not fall on the strain path. If thrusting is assumed to postdate overturning of the beds, comparison of that locality (WSRT) with WSRU suggests that all three axes were changed by the later deformation. One locality, JQ, should fall on the strain path near WSRU because it is also from an overturned fold limb. Strains at JQ, however, are significantly less (Fig. 14). The JQ locality is west of the others in garnet

grade rocks, and metamorphism culminated earlier westward. One possible explanation for the lower strains is that metamorphism may have caused pressure solution deformation to cease sooner, before appreciable deformation occurred.

CONCLUSIONS

Pressure-solution deformation has caused substantial volume redistribution within the Purgatory Conglomerate from Rhode Island. Cobble volume losses of 23% in fold hinges to 55% in overturned limbs have been documented. Real cobble strains are moderate ($e_X = 0\%, e_Y = -20$ to -37%, and $e_Z = -11$ to -42%) as might be expected for a pressure-solution deformation mechanism. Nevertheless, small axial strains produce significant volume losses. Originally oblate cobbles became prolate during this finite constrictional deformation, and most of the apparent strain is caused by the initial ellipsoidal shapes of cobbles. Much of the volumetric strain apparently occurred early in the deformation history.

Acknowledgements—The data presented in this paper comes from the author's Ph.D. dissertation which was completed under the supervision of Dr Dennis S. Wood at the University of Illinois at Urbana. Drs Mark A. Helper, Martin P. A. Jackson, Rachel J. Burks, S. H. Treagus, and two anonymous reviewers are thanked for excellent critical reviews of the manuscript. Dr Wood is thanked for his help and inspiration during the time in which the original research was conducted. Partial funding was provided by two Geological Society of America Penrose Research grants, a Sigma Xi Research Grant, and the Owen–Coates Fund of the Geology Foundation, University of Texas at Austin.

REFERENCES

Alvarez, W., Engelder, T. & Geiser, P. A. 1978. Classification of solution cleavage in pelagic limestones. *Geology* **6**, 263–266.

Cloos, E. 1947. Oolite deformation in the South Mountain Fold, Maryland. *Bull. geol. Soc. Am.* **58**, 843–918.

De Boer, R. B. 1975. Influence of pore solution of rock strength. Unpublished Ph.D. thesis, State University of Utrecht.

De Boer, R. B. 1977. On the thermodynamics of pressure solution—interaction between chemical and mechanical forces. *Geochim. cosmochim. Acta* **41**, 249–256.

Deelman, J. C. 1975. "Pressure solution" or indentation? *Geology* **3**, 23–24.

Dunnet, D. 1969. A technique of finite-strain analysis using elliptical particles. *Tectonophysics* **7**, 117–136.

Dunnet, D. & Siddans, A. W. B. 1971. Nonrandom sedimentary fabrics and their modification by strain. *Tectonophysics* **12**, 307–325.

Durney, D. W. 1972. Solution transfer, an important geological deformation mechanism. *Nature* **235**, 315–317.

Elliott, D. 1970. Determination of finite strain and initial shape from deformed elliptical objects. *Bull. geol. Soc. Am.* **81**, 2221–2236.

Elliott, D. 1973. Diffusion flow laws in metamorphic rocks. *Bull. geol. Soc. Am.* **84**, 2645–2664.

Engelder, T. & Engelder, R. 1977. Fossil distortion and décollement tectonics of the Appalachian Plateau. *Geology* **5**, 457–460.

Farrens, C. M. 1982. Styles of deformation in the southeastern Narragansett Basin, Rhode Island and Massachusetts. Unpublished Master's thesis, University of Texas at Austin.

Flinn, D. 1956. On the deformation of the Funzie conglomerate, Fetlar, Shetland. *J. Geol.* **64**, 480–505.

Flinn, D. 1962. On folding during three-dimensional progressive deformation. *Q. Jl geol. Soc. Lond.* **118**, 385–433.

Gay, N. C. 1968. Pure-shear and simple-shear deformation of inhomogeneous viscous fluids, I and II. *Tectonophysics* **5**, 211–234, 295–302.

Geiser, P. A. 1974. Cleavage in some sedimentary rocks of the Central Valley and Ridge Province, Maryland. *Bull. geol. Soc. Am.* **85**, 1399–1412.

Geiser, P. A. 1979. Present knowledge of strain distribution in the Appalachian Orogen (abstract). *Geol. Soc. Am. Abs. Prog.* **11**, 431.

Gratier, J. P. 1983. Estimation of volume changes by comparative chemical analyses in heterogeneously deformed rocks (folds with mass transfer). *J. Struct. Geol.* **5**, 329–339.

Gray, D. R. 1978. Cleavages in deformed psammitic rocks from southeastern Australia: Their nature and origin. *Bull. geol. Soc. Am.* **89**, 577–590.

Gray, D. R. & Durney, D. W. 1979. Crenulation cleavage differentiation: implications of solution-deposition processes. *J. Struct. Geol.* **1**, 73–80.

Grunsky, E. C., Robin, P.-Y. F. & Schwerdtner, W. M. 1980. Orientation of feldspar porphyroclasts in mylonite samples from the southern Churchill Province, Canadian Shield. *Tectonophysics* **66**, 213–224.

Heim, A. 1919. *Geologie der Schweiz.* Tauchnitz, Leipzig.

Helm, D. G. & Siddans, A. W. B. 1971. Deformation of a slaty, lapillar tuff in the English Lake District: discussion. *Bull. geol. Soc. Am.* **82**, 523–531.

Hossack, J. R. 1968. Pebble deformation and thrusting in the Bygdin area (southern Norway). *Tectonophysics* **5**, 315–339.

Houle, J. A. 1980. Depositional systems, sandstone diagenesis, and cobble study in the Lower Pennsylvanian Taos trough, Northern New Mexico. Unpublished Master's thesis, University of Texas at Austin.

Hsu, T. C. 1966. The characteristics of coaxial and non-coaxial strain paths. *J. Strain Anal.* **1**, 216–222.

Kuenen, P. H. 1942. Pitted pebbles. *Leid. geol. Meded.* **13**, 189–201.

Lisle, R. J. 1977. Estimation of tectonic strain ratio from the mean shape of deformed elliptical markers. *Geologic. Mijnb.* **56**, 140–144.

McClay, K. R. 1977. Pressure solution and Coble creep in rocks and minerals: a review. *J. geol. Soc. Lond.* **134**, 57–60.

McEwan, T. J. 1978. Diffusional mass transfer processes in pitted pebble conglomerates. *Contr. Miner. Petrol.* **67**, 405–415.

Mawer, C. K. 1983. State of strain in a quartzite mylonite, Central Australia. *J. Struct. Geol.* **5**, 401–409.

Milton, N. J. & Chapman, T. J. 1979. Superposition of plane strain on initial sedimentary fabric: an example from Laksefjord, North Norway. *J. Struct. Geol.* **1**, 309–315.

Mitra, S. 1977. A quantitative study of deformation mechanisms and finite strain in quartzite. *Contr. Miner. Petrol.* **59**, 203–206.

Mosher, S. 1976. Pressure solution as a deformation mechanism in Pennsylvanian conglomerates from Rhode Island. *J. Geol.* **84**, 355–364.

Mosher, S. 1977. The significance of pressure solution in conglomerate deformation. *Trans. Am. geophys. Un. (EOS)* **58**, 1239.

Mosher, S. 1978. Pressure solution as a deformation mechanism in the Purgatory Conglomerate. Unpublished Ph.D. thesis, University of Illinois at Urbana.

Mosher, S. 1980. Pressure solution of conglomerates in shear zones, Narragansett Basin, Rhode Island. *J. Struct. Geol.* **2**, 219–226.

Mosher, S. 1981. Pressure solution deformation of conglomerates from Rhode Island. *J. Geol.* **89**, 37–55.

Mosher, S. 1983. Kinematic history of the Narragansett Basin, Massachusetts and Rhode Island: constraints on late Paleozoic plate reconstructions. *Tectonics* **2**. 327–344.

Mosher, S. & Wood, D. S. 1976. Mechanisms of Alleghenian deformation in the Pennsylvanian of Rhode Island. In: *Geology of Southeastern New England* (edited by Cameron, B.). New England Intercollegiate Geologic Field Conference, 68th Annual Meeting, Boston, MA, 472–490.

Mosher, S. & Wood, D. S. 1978. Pressure solution and conglomerate deformation in Rhode Island. *Geol. Soc. Am. Abs. Prog.* **10**, 76.

Nickelsen, R. P. 1966. Fossil distortion and penetrative rock deformation in the Appalachian Plateau, Pennsylvania. *J. Geol.* **74**, 924–931.

Nickelsen, R. P. 1972. Attributes of rock cleavage in some mudstones and limestones of the Valley and Ridge province, Pennsylvania. *Proc. Pa. Acad. Sci.* **46**, 107–112.

Ramsay, J. G. 1967. *Folding and Fracturing of Rocks.* McGraw-Hill, New York.

Ramsay, J. G. & Wood, D. S. 1973. The geometric effects of volume change during deformation processes. *Tectonophysics* **16**, 263–277.

Ramsay, J. G. & Huber, M. I. 1983. *The Techniques of Modern Structural Geology: Volume* 1: *Strain Analysis.* Academic Press, New York.

Ribeiro, A., Kullberg, M. C. & Possolo, A. 1983. Finite strain estimation using 'anti-clustered' distribution of points. *J. Struct. Geol.* **5**, 233–243.

Rust, B. R. 1972. Structure and process in a braided river. *Sedimentology* **18**, 221–245.

Schwerdtner, W. M. 1982. Calculation of volume change in ductile band structures. *J. Struct. Geol.* **4**, 57–62.

Siddans, A. W. B. 1983. Finite strain patterns in some Alpine nappes. *J. Struct. Geol.* **5**, 441–448.

Sorby, H. C. 1853. On the origin of slaty cleavage. *Edinb. New Philos. J.* **55**, 137–148.

Sorby, H. C. 1863. On the direction correlation of mechanical and chemical forces. *Proc. R. Soc.* **12**, 538–550.

Von Plessmann, W. 1964. Gesteinslösung, ein Hauptfactor beim Schieferungsprozess. *Geol. Mitt.* **4**, 69–82.

Walker, R. G. 1975. *Conglomerate: Sedimentary Structures and Facies Model*. Soc. Econ. Paleontologists and Mineralogists Short Course No. 2, 133–161.

Wood, D. S. 1973. Patterns and magnitudes of natural strain in rocks. *Phil. Trans. R. Soc. A* **274**, 373–382.

Wood, D. S. 1974. Current views on the development of slaty cleavage. *Annu. Rev. Earth & Planet. Sci.* **2**, 369–401.

Wood, D. S. & Oertel, G. 1980. Deformation in the Cambrian slate belt of Wales. *J. Geol.* **88**, 285–308.

Wright, T. O. & Platt, L. B. 1982. Pressure dissolution and cleavage in the Martinsburg Shale. *Am. J. Sci.* **82**, 122–135.